EPH - International Journal of Mathematics and Statistics
ISSN (Online): 2208-2212
Volume 4 Issue 1 February 2018

DOI:https://doi.org/10.53555/eijms.v4i1.16

NOISE THEORITICAL INVESTIGATIONS FOR TRI-DIMMENSIONAL NMR CIRCUIT: TOWARDS THE NANOSCALE

Yue Ma[1], Samir Labiod[2], Latifa Fakri-Bouchet[3], Jacques Verdier[4], Francis Calmon[5], Saïda Latreche[6] and Christian Gontrand[7*]

*[*1,3,4,5,7]Institut des Nanotechnologies de Lyon, Université de Lyon, INSA- Lyon, CNRS-UMR5270, Villeurbanne, F-69621,FRANCE.*

[2]LHS Université Mentouri, ALGERIA

[7]Département Génie électrique, Université Euro-méditerranéenne de Fès, INSA - Fès Route de Meknès, BP 51 - 30 070 Fès, MAROCO

Corresponding Author:-

Email: Christian.Gontrand@insa-lyon.fr

Abstract:-

In recent years, NMR/MRI portable devices have drawn attention of numerous researcher teams. They are used for variety of applications, from medical diagnosis to archaeological analysis, nondestructive material testing evaluation of water presence in building materials and food emulsions. Different magnets designs have been proposed by many groups of research. They can be divided into two groups: the magnets ex-situ and the magnets in situ .The first group has the simple configuration with the sensitive volume near their surface and the samples under test are located outside the magnets. Thus, they can be used for the experimental investigation of objects with any dimension. Although the ex-situ magnets have simple shape and light weight, they are difficult to achieve in terms of homogeneity of the magnetic field in the sensitive volume.

In comparison, the in-situ magnets have their static field reinforced inside their bore center and canceled outside of the structure. Thus, their magnetic field is roughly homogeneous inside the structure.

But drawbacks still exist and can be amplified, especially the in depth problem of Signal/Noise. Calculations, in a microscopic point of view, are develop, first applied to resistances and inductances imbedded in this circuit.

Before, from any point source, we calculate the impedance spreading out. For this, our approach is using Transmission Line Model, over or into a multi-layered substrate; it can be also derived by solving Poisson's equation analytically to obtain the associated Green's kernel. We implement our algorithms in MATLAB. Thus, it permits to extract impedances between any two embedded contacts, real or virtual, of any shape or thickness.

I. INTRODUCTION

Substrate noise coupling in integrated circuits becomes a significant consideration in the circuit design. Nowadays, micro (nano) technology and the development of semiconductor technology enable designers to integrate multiple systems into a single chip, not only in 2D (planar), but also in 3D (in the bulk). This design technology reduces cost, while improving performance and makes the possibility of a system to be on chip [1]-[2].

3D Si integration seems the right way to go and compete with Moore's law (more than Moore *versus* more Moore). However, it is still a long way to go.

In 2010, the question was: Why 3D? Today, the questions are: When 3D? and How to use 3D? The 3D chip stacking is well known to overcome conventional 2D-IC issues, using indepth contacts or some through silicon for signal transmission.

The kind of silicon substrate in which 3D interconnections are processed is an important parameter and has a strong impact on 3D interconnection electrical behavior .Electrical modeling methods are dependent on the substrate type of the application. Two different kinds of P silicon substrates are typically used in CMOS/BiCMOS processes: uniform lightly doped substrate (>1Ω.cm) and heavily doped substrate (<1Ω.cm) with lightly thinned doped (>1Ω.cm) epitaxial layer. Other semiconductor substrates are used in micro/nano technologies *and could embed 3D interconnections (SOI technologies, MEMS technologies, sensor technologies…).*

Indeed, we attempt to propose a beginning of synthesis of electrical and noise phenomena studies in 3D layered circuits. First of all, we can solve Poisson's equation, using Green Kernels [3]-[5]; this mathematical method is an analog to the Transmission Line Matrix (TLM) , based on reflection-transmission of voltage and current through the layers, when adapting it to embedded contacts of any shape.

On another hand our demonstrator of predilection concerns NMR (see fig 1[7]:,^ the MNR system, and fig.2 concerning the pre-study of the substrate, using FEM methods [8], as well as the 3D device ; substrate with embedded connectics and circuits; two aligned coils are used for the detection accuracy: safety against noise or parasitic signals. Nuclear magnetic resonance (NMR) is a resonant interaction between a radio-frequency (RF) magnetic field and the nucleic magnets placed in a static magnetic field. Since the detailed resonance behavior is influenced by the environment of the nucleic magnets, NMR can be used for biomolecular sensing, medical imaging: our subject of predilection.

The benefits of NMR would be broadly available, if NMR instruments can be made small and at low cost. Nonetheless, NMR systems remain bulky, heavy, and expensive. An NMR system consists of a magnet to produce (fig1):

- a static magnetic field,
- one coil (or more)
- an RF transceiver to generate an RF magnetic field and to monitor the resonance.

Since a larger-sized magnet tends to yield a stronger NMR signal, even for the same static field strength and hence relaxes the sensitivity requirement on the transceiver design, large magnets are used, where the magnet is by far the largest component.

To use a small magnet, then to detecting the NMR signal weakened, our aim leads to develop: A quasi fully integrated, high-performance CMOS RF transceiver and a separate high-quality planar coil(s).

- Heterodyne Receiver With Passive Amplification (Fig.3)

The receiver consists of a low noise amplifier (LNA), a variable gain amplifier (VGA), mixers and switches, The noise figure (NF) of the receiver have to be minimized. To this end, both minimization of the LNA's input referred noise and optimum LNA-coil noise matching are necessary. To minimize the LNA's input referred noise, we use for the LNA some resistive loads (in place of active loads); Then, no common-mode feedback circuit is needed. In the same time noise sources are reduced.

To compensate the low gain induce the passive loads, we use a three -stage amplifier; 2) PMOS transistors are used as input devices to minimize noise (imput surfaces are notable) and substrate coupling from digital circuits. Using a cascode configuration give a supplement degree of liberty (independent currents in the branches), then attenuating coupling between the local oscillator and the LNA.

The filter acts as a low noise preamplifier with "passive" voltage gain of since the LNA's input impedance is much larger than that of the coil.

. As it has negligible loss compared to the coil, the passive amplification hardly adds any noise and maintains the original signal-to-noise-ratio (SNR) from the coil. In other words, the passive amplifier has an NF near 0 dB but with the low gain of, which leads to a low receiver noise figure. Howevern this passive amplification scheme is not applicable for wideband:

But it suits well the NMR signal, which in general has a very narrow bandwidth (a few kHz). Nonetheless, non-optimal coil-LNA impedance matching at 50, instead of the optimum noise matching based on the passive amplification, has been a conventional choice.. This shows an advantage of the integrated NMR electronics. The LNA-coil resonance matching for minimum noise figure corresponds to an impedance mismatch between the LNA and the coil. In contrast, the Power Amplifier and the coil need to be impedance matched In order to simultaneously achieve both the optimum LNA-coil noise matching and PA-coil power matching…right].

Hence, in this paper, we deal essentially on electronic noise , redhibitory in such a complex system, addressing some theoretical insights on this purpose.

MATHEMATICAL TOOLS

In this paper, Green functions are applied to homogeneous stacked layers for substrate circuit model extraction, as opposed to numerical methods; the resolution speed of the former method is much faster. Some basic recalls and concepts are first introduced. The use of discrete cosine transforms (DCT), applying twice a FFT - Fast Fourier transform - in this model, will accelerate and compute the speed. Then, an improved model, which can be applied on substrate with in-depth contacts (or via), is shown; it can treat the case of contacts lying in different layers.

For verification, we compare with a finite element method (FEM) [6].

The high density integration and high system frequency make substrate noise coupling become one of the most significant considerations in the design due to its great impact on the performance of ICs. The aim of this 3D substrate analysis is, first of all, to efficiently extract the Z impedance parameters between any contacts (electrode, *via*) which are located on or into the silicon substrate. An efficient impedance extraction tool, for any two contacts, could help the designer to accelerate the design and optimize the final layout. Like in planar technologies, 3D interconnects can be built as an 'RLCG' - divider bridge: (G//C)/ (R series L) - equivalent electrical model, with a Π or a T network. Often, a simple compact model is constructed by modeling the substrate as a simple node. However, this assumption is only viable when substrate is highly conductive, in low and medium frequency domains, and is not suitable for the multi-layer substrates. That is the reason why, in this paper, we propose a substrate extraction method relying on Transmission Line Matrix method (TLM) over multi-layered substrate and/or Green functions to model these effects, in the bulk [3].

A. Substrate Analysis

The most well-known pioneering paper came from Gharpurey [3]: a layered 3D substrate, with 2 surface contacts (Fig 4. a) and 4.b)):

We present hereafter a 3D substrate study with top or embedded contacts. The originality as we consider and apply here is to do all the calculations in the reciprocal domain, from the very beginning of the calculations to the end, to extract voltage or temperature.

Generally, the Z parameters could be defined as:

$$Z_{mn} = \left.\frac{V_m}{I_n}\right|_{I_{k\neq n}=0} \tag{1}$$

In practical operation, by injecting a unitary current as an excitation source, I at the *n*-th point, and a unitary current excitation source, - I (equivalent to a sink current I) at an m-th point and calculate the resulting voltage at the probe point, we can get the direct impedance Zmn between the m and n contacts.

If we can get the resulting potential distribution in the substrate caused by the unitary current, we could get easily the Z parameters by (1).

Under quasi-static conditions, the potential over the substrate satisfies Laplace's equation

$$\nabla^2\varphi(x,y,z)=0 \tag{2}$$

It can also be written as:

$$\left(\frac{\partial^2}{\partial x^2}+\frac{\partial^2}{\partial y^2}+\frac{\partial^2}{\partial z^2}\right)\varphi(x,y,z)=0 \tag{3}$$

Hereafter, for Poisson or heat diffusion equations, the analytical method is, first of all, based on the algorithm of variable separation, leading to solve an eigen problem.

We assume that = X (x,□x'). Y (y, y'). Z (z, z'), we can rewrite (3) [4 - 6]

By defining:

$$Z(z,z') = Z'(z,z')\cdot\cos\left(\frac{m\cdot\pi\cdot x'}{a}\right)\cdot\cos\left(\frac{n\cdot\pi\cdot y'}{b}\right) \tag{4}$$

And we get, for a potential due to a point charge, a simple equation:

$$\frac{ab}{4}\cdot\left[\frac{d^2Z}{dz^2}-\gamma_{mn}{}^2\cdot Z\right]=-\frac{\delta(z-z')}{\varepsilon_N}\ \text{with}\ \gamma_{mn}=\sqrt{\left(\frac{m\cdot\pi}{a}\right)^2+\left(\frac{n\cdot\pi}{b}\right)^2}=\sqrt{(\lambda)^2+(\mu)^2} \tag{5}$$

For $z \neq z'$, □ $(z-z') = 0$. The above equation, (5), has a well-known general solution:

$$Z' = A\cdot e^{-\gamma_{mn}\cdot(d+z)} + B\cdot e^{\gamma_{mn}\cdot(d+z)} \tag{6}$$

This equation above invokes also a transmitted wave and a reflected one.

Then, it seems to us most graspable to use the well-known paradigm of the Transmission Line Matrix method, for clarity, that developing a more formal mathematical method based on Green kernels. And this physical approach is easier for understanding.

-Transmission Line Analogy for Multi-Layered Media

In its simplest form, a transmission line is a pair of conductors linking together two electrical systems (source and load, for instance), with a forward and return paths; for cases where the return path is floating, a third conductor (or more) is introduced as the grounding shield. For microwaves, they are waveguides. In our case, the propagation of EM waves, their interferences, through the silicon substrate, is among the most serious obstacles in the steady trend towards integration of present day microelectronics. In fact the TL method (TLM) has been established in some cases concerning substrate surfaces; TLM can be seen as a more physical interpretation of the mathematical developments presented above. The principal strength of this method seems to be well dedicated to embedded contacts, irrespective of their number and shape.

Let us consider a plane wave through a multi-layered medium, its plane of incidence being parallel to the <x,y> plane, providing the same boundary conditions as mentioned above.

Then, we consider the general case in which the line's impedance is not the same as that of the load. A wave front A hits the load Z_L: a part of energy is absorbed by Z_L, the remaining energy is reflected; in this case, voltage and current wave-fronts are not in phase. This reflected wave can meet another incident wave front B.

The direction of the current flow depends on the polarity of the waveform at the time of observation; if two positive directed waveforms (one forward an one reflected) meet, the current waveforms subtract but the voltage waveforms add. Likewise, if a positive directed waveform meets a negative directed waveform, the current will add and the voltage will substract.

The expression for the apparent impedance is given below:

$$Z = \frac{V_{total}}{i_{t\,otal}} = \frac{V_F \pm V_R}{i_F \mp i_R} \qquad (7)$$

Then, the general solution for voltage and current is:

$$V(z) = V_f e^{\gamma z}\, V_r e^{-\gamma z} \qquad (8)$$

$$I(z) = Y_c(V_F e^{-\gamma z} - V_r e^{\gamma z}) \qquad (8bis)$$

Where the propagation coefficient is the square root of the product Z by Y, the linear impedance and admittance, respectively;

□□□□□□□□□□□□□□□attenuation, □□360°/□$_{si}$.

Deriving directly from the chain matrix:

$$\begin{bmatrix} V_1 \\ I_1 \end{bmatrix} = \begin{bmatrix} \cosh \gamma L & Z_c \sinh \gamma L \\ Y_c \sinh \gamma L & \cosh \gamma L \end{bmatrix} \begin{bmatrix} V_2 \\ -I_2 \end{bmatrix} \qquad (9)$$

and from the output branch: $V_2 = - Z_L I_2$, we get:

$$\begin{bmatrix} V_1 \\ I_1 \end{bmatrix} = -I_2 \begin{bmatrix} Z_L \cosh \gamma L & Z_c \sinh \gamma L \\ Z_L Y_c \sinh \gamma L & \cosh \gamma L \end{bmatrix} \begin{bmatrix} 1 \\ 1 \end{bmatrix} \qquad (10)$$

where $Z_c = 1/ Y_c$ (square root of Z and Y ratio) is the characteristic impedance (Electric and magnetic fields modulus ratio), Z_L is the charge impedance, L is the distance from the load; we can extract an input impedance, Z_l ($=V_1/I_1$), function of the load impedance Z_{l+1} (l: layer number) as:

$$Z_l = Z_c \frac{Z_{l+1} + Z_c \tanh \gamma L}{Z_c + Z_{l+1} \tanh \gamma L} \qquad (11)$$

In fact, restarting from (7), taking into account the limit or boundary conditions – continuity of potential, and discontinuity of the electric field if there is a surface charge at the considered layer interface – it is easy to program this iterative solution against substrate depth, or layers of eq.(7).

In fact, these calculations are made only one time, at each frequency.

In our simulator, using MATLAB [9], we use a matricial formalism, extending the impedance (Z) and the current (T) transmission from a layer l to its adjacent one (cf. (9) or (17)), starting from a k layer:

$$\begin{bmatrix} Z_{k,l+1} \\ T_{k,l+1} \end{bmatrix} = \begin{bmatrix} A_k & -B_k \\ C_k & -D_k \end{bmatrix} \begin{bmatrix} Z_{k,l} \\ T_{k,,l} \end{bmatrix} \qquad (12)$$

Where T addresses the derivation of the current (between two parallel regions)

The ABCD-parameters are known variously as chain, cascade, or transmission line parameters.

This cascade connection model is very suitable.

As mentioned earlier, all the calculations are done in the reciprocal space. For instance, the potential is derived from the (kronecker) product of (sub-) matrix Z, by a DCT of the matrix of the injected current, accomplished using two consecutive FFTs.

In our algorithm, the contact voltage is the mean value of the voltage of the discrete contact elements, calculated *via* Millman's theorem, as:

$$V = \frac{\sum_{n=1}^{N} j\omega c\varphi_n}{\sum_{n=1}^{N} j\omega c} = \frac{1}{N}\sum_{n=1}^{N}\varphi_n \qquad (13)$$

Where φ_n is the substrate voltage at a node and N is the number of contact sub-areas. So, in our modified algorithm, the contact voltage is then calculated by taking the average <Va> of the potentials of the substrate region, under the injecting contact.

II. TLM RESULTS

In this paper, as a check, a typical process flow compatible BiCMOS 0.35 m technology is first considered; on Fig. 4.a, a specific region (P^+/P) of this process is presented.

We approximate the actual profile by stacked layers of given thicknesses (taken *ex abrupto*) uniformly doped Fig. 4.b.

First of all, we did some numerical experiences (not presented here) using COMSOL [8], a well-known multiphysics (cf. electrical, thermal, mechanical couplings) simulator, for testing its robustness and accuracy; it is also a dedicated tool for full wave electromagnetic analysis. It uses essentially Galerkin-like algorithms; typically, a 3D simulation can use a few ten of minutes or more than one hour.

- Contacts Embedded

Considering the general case were the contacts (previous works exist for surface contacts [3]), real or virtual, are totally embedded. Then, the substrate can be seen as an actual parallel connection of two separated parts (current derivation). The current is injected on a contact of an i^{th} layer, so the substrate is divided in two parts, from this layer.

We write a synoptic model algorithm, all developed in the reciprocal spaces in.

Now, it seems easy to calculate any transfer impedance by TLM. Possibly embedded in the substrate, contacts can be introduced into any layer; they can be real (*e.g.*: metal like) or virtual, of any shape.

The surface die is typically 30 *m**30 *m*, with M=N=300; surface contact: 20 points by 20 points (the calculation points, M*N, are equidistributed).

We present in the Fig. 5 the the impedance between some Ci and Cj contacts, at the interfaces L_3/ L_4 and L_7/ L_8; it is typical of a Lorentzian curve (R//C, with R.C=; the comparison between "TLM/Green" and "COMSOL" is quite good. Moreover, in Fig. 5,, from our 3D-TLE - Transmission Line Extractor -simulator and COMSOL for a 12 layers substrate, at the frequency of 100GHz, are quite similar. Still, a very good accordance was showed between FEM and TLM; since calculations are made with current source, then, we get voltage variation under contacts.

From above results one can find that the comparison between "TLM/Green" and "COMSOL" is quite good. The proposal method calculated results agree well with the COMSOL simulation ones, while our method uses comparatively less time (roughly 1/50 to 1/100).

The potential distribution of the two contacts model obtained, one can find the potential on the contact surface is not uniform (high voltage region). The non-uniform potential is caused by an injection of uniform current density instead of a uniform voltage. This non uniform potential feature makes 3D-TLE very profitable when one calculates the impedance of two resistive regions rather than two metal contacts, for example, the oxide-insulated conductive regions (*e.g.* pads and coplanar waveguide) and junction-insulated well regions (*e.g.* n-well regions over a p-type substrate). In these cases, the substrate plates could not be considered as an equipotential plate.

The simulation results obtained with Green/TLM (fig.5) implemented in MATLAB and compared with COMSOL are found to be practically equal. Indeed, we choose, in MATLAB, layers as perfect parallelepipeds (uniform thickness layers); in this event, the so called eq. (6) is an exact analytical solution. Otherwise, with refined meshes concerning the FEM methods, the solution convergence is unique. If we design layers with some thickness variation, the two methods will not present exactly the same solutions, depending on this variation, because eq(8) is no more an exact solution.

- Generation_Recombination processes

Accordingly, the G-R noise represents a typical, and fundamental, noise source in semiconductor materials and devices, where carrier concentration can vary over many orders of magnitude. For electron fluctuations occur between two levels: conduction band and donor impurity. Conductivity, associated to GR noise, can be written as a low frequency first order transfer function, with an associated carrier life time, as:

$$\sigma_{GR} = \frac{\sigma_0}{1+j\omega\tau} \qquad (14)$$

We present two first examples as checks (cf Figure 5).

a) *"Bad "contact* only under the contact C4, at its base, in the L4 4th layer whole depth, we consider theGR noise.

b) In the L6 6th whole layer, we consider also the same GR noise. The result are depicted; in figure 6.a and 6.b, respectively.

We observe clearly, on both cases, the influence of the added GR current, lowering the resistance at low frequencies, before a cut-off frequency f_c=1/ (2. The impedance, for a lifetime of 1ns, can decay from 5% from its reference value without GR.

These first qualitative, but also quantitative results, seem us important; for instance: injecting at the upper contact a Generation-Recombination-like noise, and probing at the lower one contact, we could extract a possible lorentzian frequency response, with a cut-off frequency, signature of the G-R process

As we suggested, this method (« Green/TLM ») can be linked to the so called impedance transfer method [11, 12], considering signal fluctuations; injecting a current variation at a contact creates a potential variation at any another contact (Fig.7). This way, we could analyze possible correlations between different, *ab initio*, independent noise sources [13], for instance considering the nano-scale.

Our present work will be also to consider quadratic forms ; the transfer impedance method, a proper two-point internal response function, gives a linear relation between the electricfield response and a local current perturbation, thus, enabling one to compute the internal field noise spectra, originated from current fluctuations. This method, by generalizing the original impedance field method of Shockley et al [11] has been widely used during the last decades for noise calculations, but in one dimension. The essential role of the TLM was, and nowadays is, to calculate the total spectrum of voltage fluctuations between the terminals of a one-port device (Fig.7). Currently, no new insights permit to solve this problem in three-dimensional dimensions (even in 2D), not because of numerical difficulties, but in a sound physical point of view.

- Application example: noise in ohmic space charge regime (simple injection)

The sample is assumed to be a parallelepiped; we are dealing with a longitudinal unidimensional case. The space charge in not negligible and can make the device's characteristics nonlinear. We distinguish between the two different regimes:

a) When the space charge of the injected carriers is very weak to significantly affect the volume's conductivity, we get the ohmic regime, where the mean current is proportional to the voltage appmied at the junctions of the sample: $l_o \propto V_o$.

$$j = -q\mu n E + \varepsilon \frac{\partial E}{\partial t} \quad (15)$$

$$\frac{\partial E}{\partial x} = \frac{-q}{\varepsilon}(n - N_D) \quad (16)$$

$$j_n(\vec{r},t) = e\,\mu_n E\left(N_D + \frac{\varepsilon}{e}\frac{\partial E}{\partial t}\right) + \varepsilon\frac{\partial E}{\partial t} \quad (17)$$

(q = -e, >0)

Consider, now, fluctuations(Fig.7):

$$E = E_0 + \square\, E\, e^{i\square t} \quad (18)$$

$$n = n_0 + \square\, n\, e^{i\square t} \quad (19)$$

$$j = j_0 + \square\, I\, e^{i\square t} \quad (20)$$

$$\Delta j_n(\vec{r},t) = e.N_D\,\mu\Delta E) + \varepsilon\mu\ E_0\frac{\partial \Delta E}{\partial x} + \varepsilon\mu\ \Delta E\ \frac{\partial E_0}{\partial x} + i\varepsilon\omega\Delta E \quad (21)$$

Hence:

$$\varepsilon\mu\ E_0\frac{\partial \Delta E}{\partial x} + (e\,\mu\ N_D + \varepsilon\mu\frac{\partial E_0}{\partial x} + i\varepsilon\omega)\Delta E = \Delta j_n \quad (22)$$

If $n=N_D$ (at the ambient, for example)

$$\varepsilon\mu E_0\frac{\partial \Delta E}{\partial x} + (-e\,\mu_n + i\varepsilon\omega)\Delta E = \Delta j_n \quad (23)$$

$$\varepsilon\mu E_0\frac{\partial \Delta E(x,x')}{\partial x} + (e\,\mu\ N_D + i\varepsilon\omega)\Delta E'x,x') = \Delta j_n \quad (24)$$

The solution is:

$$\Delta E(x,x') = \frac{\Delta j_n}{-e\,\mu_n + i\varepsilon\omega} + K(x)e^{-\frac{e\,\mu_n N_D + i\varepsilon\omega}{\epsilon\mu_0 E_0}x'} \quad (25)$$

$$\Delta E(x,x') = \frac{\Delta j_n}{e\,\mu_n + i\varepsilon\mu\omega} + \left(1 - e^{\frac{e\,\mu N_D + i\varepsilon\mu\omega}{\epsilon\mu_0 E_0}(x - x')}\right) \quad (26)$$

The impedance gradient is defined by:

$$\frac{\partial Z(N,x)}{\partial x} = -\frac{1}{\Delta I}\int_x^L \frac{\partial \Delta E(x,x'))}{\partial x}dx' \quad (27)$$

So the diffusion length is much smaller than that of the sample, we can write:

$$\frac{\partial Z(N,x)}{\partial x} = \frac{\Delta j_n}{S(\,i\varepsilon\omega^{\circ}\, e\,\mu_n)} .(1 - e\frac{e\,\mu \quad N_D + i\varepsilon\omega}{\epsilon\mu_0 E_0}^{(x-L)})(28)$$

As for the noise,

$$\frac{\partial Z(N,x)}{\partial x} = \frac{\Delta j_n}{S(\,i\varepsilon\omega \mp e\,\mu_n D)}(29)$$

Using the Einstein relationship, kT/q = D/, (30)
We get:

$$S_v = 4e^2 D\mu.\frac{nL}{(S\varepsilon\omega)^2+(Se\,\mu N_D)^2} \quad (31)$$

Finally,

$$S_v = 4kT\frac{R}{1+(\omega RC)^2}(32)$$

It is the noise of a parallel RC circuit (cf. above – first order electrical calculations for buried layers modeling the substrate out of the nanoscale.
Where C= □ S/L (33) and R= L/ (q □ nS) (33 bis)

-Generation—Recombination noise
In a semiconductor, new carriers can be generated, in a N quantity; by illuminating, for instance. If is the life duration, we can write:

$$\frac{d\Delta n}{dt} = -\frac{\Delta n}{\tau}(34)$$

Now, considering fluctuations [13]:

$$\frac{d\Delta n}{dt} = -\frac{\Delta n}{\tau} + N(t) \quad (35)$$

If the source is harmonic:

$$N(t) = N_0 e^{j\omega t} \quad (36)$$

so is□□n (cf. linearity) : $\Delta n(t) = \Delta N e^{j\omega t}$ (37)

Finally :

$$S_N(f) = S_{\Delta n}(f)\left|\frac{1}{\tau} + j\omega\right|^2 (38)$$

If the noise is white,

$$<\Delta N^2> = \int_0^{\infty} S_{\Delta N}(f)df = S_N \tau^2 \int_0^{\infty} \frac{1}{1+4\pi^2 f^2 \tau^2} df = S_N \frac{\tau}{4}(40)$$

Hence:

$$S_{\Delta N}(f) = 4 <\Delta N^2> \frac{\tau}{1+\omega^2\tau^2} \quad (41)$$ Fig.8

The spectrum is known if $<\Delta N^2>$ is; then, we deal with a master equation addressed to microscopic phenomena.
V is a complex voltage (cf. harmonic régime), superposed to the quiescent point, continue, induced par I.

- The coil L, modeled by a circuit (L, R), with the noise current spectral density in this circuit, is traversed by a mean current zero. We insert for this the perfect circuit, a noisy source □ (t) and the circuit obeys the equation;

L di / dt + Ri = v (t) (42)

In harmonics,
That is: $v=V_m.e^{j\,t}$ (43) and t $i=I_m.e^{jt}$(43bis) □
The result is well known:

$V_m = Z\, I_m$ (44), avec Z=R+jl □ □ whre Y est the admittance Y = 1/Z. (45) Hence:

$S_V(f) = |Z|^2 S_I(f)$ (46)

$$S_I(f) = \frac{S_V(f)}{R^2 + L^2\omega^2} \quad (47)$$

Now consider the microscopic aspect and calculate $<i^2>$.

The inner mean energy, into th coil, is: ½.Li² For 1D, we can write:

½.Li² =½.kT (48)

Moreover:

$$< i^2 >= \int_0^\infty S_i(f)\ df\ ) = \int_0^\infty \frac{df}{R^2 + 4\pi^2 L^2 f^2} \quad (49)$$

$$= \frac{S_V}{4RL} (49)$$

Then:

$S_V = 4kRT$ (cf. Johnson–Nyquist theorem) (50)

$$S_I = 4kT \frac{R}{R^2 + L^2\omega^2} (51)$$ - See fig.9 -

- *Case of several noise sources* (Fig.10)

Noise with two sources:

$$E_n = E_{n2} + E_{n1} \cdot \frac{1}{1 + (j\omega R_1 C)} (52)$$

$$E_n E_n^* = E_{n2} + E_{n2} \cdot \frac{1}{1 + (j\omega R_1 C)} + \left(E_{n1} \cdot \frac{1}{1 + (j\omega R_1 C)}\right)^* (53)$$

$$E_n E_n^* = E_{n2} E_{n2}^* + E_{n1} E_{n1}^* \cdot \frac{1}{1 + (j\omega R_1 C)^2} \cdot + \left(E_{n2} E_{n1}^* \cdot \frac{1}{1 + (j\omega R_1 C)^2}\right) + E_{n1} E_{n2}^* \cdot \frac{1}{1 + (j\omega R_1 C)^2} \quad (54)$$

If the two noise processes are independent (hypothesis to be discussed for the nanoscale); and thermal:

$En1En2* = En2En1* = 0$ (55)

And we have:

$$S_{En} = 4kR_1T \frac{1}{1 + (\omega R_1 C)^2} + \frac{S_{En2En2}(f)}{R_2{}^2 + L^2\omega^2} = 4kR_1T \frac{1}{1 + (\omega R_1 C)^2} + 4kR_2T \quad (56)$$

-Spiral coil modeling

Considering the NMR; the coil is a key component, especially concerning its Q quality factor and its thermal noise.

A spiral inductance (Fig.11) can be regarded as an assembly of several microstrip lines. These last are very widespread in the field them radio frequencies to carry out values of a few tens of nH. In order to adapt them to the applications requiring low powers, one must increase the section of the conductor to reduce his resistance. This type of inductance is very useful in ultra-high frequency (oscillator application). The simulation is very important because it determines the characteristics of inductance to use in this type of circuits

For well characterizing an inductive bond, it is imperative to determine the value of inductance with accuracy; for this, we will model a spiral inductance in the static and frequential domains. The figure (11) shows a sight in prospect for a spiral designed with software COMSOL. The thickness of inductance is 1 µm with a width of 40 µm, the distance from separation between the whorls is 2 µm.

Figure 11.b. presents a cartography of the electrostatic potential on all the polarized structure. To calculate the value of the inductance of the model considered, it is initially necessary to solve the Poisson's equation to have the electrostatic potential on all the structure, then to solve the equation of the magnetic field for a current I cf. Ampere's theorem) We estimate the value of inductance for a thickness of 1 µm at 1.102 nH, but using software HFSS [16] we find the value 1,31 nH, this comes from the lack of smoothness of the grid at the time of the passage in finite elements. We carry out a simulation of the parameters S and the admittance on a beach of frequency of 5 MHz up to 100 GHz. The results obtained are presented on the figure (12) and are validated with those obtained by software HFSS. We could determine the value of inductance as well as the factor of quality Q in (figure (13) starting from the estimate of the Y_{11} admittance:

$$L_{11} = -\frac{1}{2*\pi*f*Im(Y_{11})} \quad (57)$$

$$Q_{11} = \frac{Im(Y_{11})}{Re(Y_{11})} \quad (58)$$

The L_{11} inductance, presents three peaks of values goshawks of the three frequencies 13.7 GHz, 52.3 GHz and 65.2 GHz. In addition, the factor of quality of inductance is maximum for the frequency 24.4 GHz. According to these results obtained, we note that there are several values of inductance in ultra-high frequency in comparison with the static result (only one value).

L_{11} inductance Fig.12), presents three peaks of values goshawks of the three frequencies 13.7 GHz, 52.3 GHz and 65.2 GHz. In addition, the factor of quality of inductance is maximum for the frequency 24.4 GHz.

So, future research is required for 3D circuits. A very true novelty, we think is to calculate transfer impedance, considering effectively the noise sources in three dimensions.

The unitary concept of spreading impedance embraces two fields in the frequency domain: electrical and noise. In the near future, to make our work more powerfull, we should consider the study of tridimensional noise couplings, and the possible correlations between noise sources, especially at the nano-scale. The major aim of this work, which seems to present some originality, also on a synthesis point of view, will be to construct some electrical global model, of the first and second order, for compact modeling of 3D circuits, an attractive multi-domain field for the industry.

- CONCLUSION

Starting from a real deal, concerning the miniaturization of a NMR sensor, we engage ourselves to a theoretical study addressed to this downscale, particularly on noise sources and their possible couplings. After simulating the circuit substrate as stacked uniformly doped layers; after extracting parallel resistance-capacitor cell for each layer, we have to take into account the layers noise.

The unitary concept of spreading impedance embraces two closed fields in the frequency domain: the electrical one and noise. In the near future, to make our work more powerful, we should consider the study of tri-dimensional noise couplings, and the possible correlations between noise sources, especially at the nano-scale. The major aim of this work, which seems to present some originality, also on a synthesis point of view, will be to construct some electrical global model, of the first and second order, for compact modeling of 3D circuits, attractive multi-domains.

Whishing down scaling our apparatus, we do some insights into noise dedicated ta nanoscale, indicating that noise sources can then be correlated although they are independent

Moreover, we perform also coil modeling, using FEM simulations in the radiofrequency domain; by now, its size reduction is not considered.

Future research is required for 3D circuits. A very true novelty, we think, will be to calculate transfer impedance, considering effectively the noise sources in three dimensions.

Acknowledgement:

- This work is supported by **UPM** (Union pour la Méditerranée)

REFERENCES

[1]. L. Di Cioccio, P. Gueguen, F. Grossi, P. Leduc, B. Charlet , M. Assous, A Mathewson, J. Brun, D. Henry, P. Batude, P Coudrain, N Sillon, L Clavelier, G Poupon, M Scannell, ‘’3D Technologies at CEA-Leti Minatec’’, 4th Int. Conf. and Exhibition on Device Packaging, IMAPS, Scottsdale (2008).

[2]. K. Banerjee, S.J. Souri, P. Kapur, and K.C. Saraswat, “3-D ICs: A Novel Chip Design for Improving Deep-Submicrometer Interconnect Performance and Systems-on-Chip Integration” in Proceedings of the IEEE, Vol. 89, No. 5, pp. 602-633, May 2001.

[3]. Ali M. Niknejad, Ranjit Gharpurey and Robert G. Meyer, “Numerically Stable Green Function for Modeling and Analysis of Substrate Coupling in Integrated Circuits,” IEEE Transactions on Computer-Aided Design of Integrated Circuits and Systems, Vol. 17, No.4, pp 305-315, April 1998

[4]. Nishath K. Verghese and David J. Allstot, “Rapid Simulation of Substrate Coupling Effects in Mixed-Mode ICs”, IEEE Custom Integrated Circuits Conference, pp18.3.1- 18.3.4, 1993. [5] Torabian, A. and Y. Chow, “Simulated image method for Green's function of multilayer media”., IEEE transactions on microwave theory and techniques, 1999. 47(9): p. 1777.

[5]. Yue Ma, Latifa Fakri-Bouchet, Francis Calmon and Christian Gontrand, ‘Electrothermal “Modelling for Three-Dimensional Nanoscale Circuit Substrates; Noise.”(cf. INFIERI) ; IEEE Transactions on Components, Packaging and Manufacturing Technology,Vol 6, N°7, juin 2016

[6]. J.Trejo Rosillo, “Contribution à l’amélioration de la sensibilité d’un micro-récepteur RMN implantable”, PhD. Thesis, n° 264-2014, Nov. 2014, Université Claude Bernard – Lyon

[7]. COMSOL Multiphysics, http://www.comsol.com/

[8]. SENTAURUSn TCAD - Synopsys, Synopsys **Sentaurus** Device, https://www.synopsys.com/silicon/tcad/device-simulation/sentaurus-device.ht

[9]. MATLAB, **MATLAB** - MathWorks, https://www.mathworks.com/products/matlab.html
[10]. A.van der ziel Noise in solid state devices and circuits ,John wiley & sons, (1986)
[11]. Van Vliet, K. M., Friedmann, A., Zulstra, R.J;J; , Gisolf, A., Van Der Ziel. A., "Noise in single injection diodes. I. A survey of methods ; J. Appl. Phys., 46, 1975, 1804.
[12]. Special issue on fluctuation phenomena, in electronic and, photonic device, IEEE Trans. On Electron devices (1994), 41.
[13]. W.Shockley, J.A.Copeland, R.P.James, Quantum Theory of Atoms, Molecules and Solid State, ed. P.O.Löwdin, Academic Press New York (1966), pp537-563.
[14]. P. Langevin, Compt.Rend, 146, 530, 1908
[15]. HFSS, ANSYS **HFSS**: High Frequency Electromagnetic Field Simulation, http://www.ansys.com/products/electronics/ansys-hfss/hfss-capabilities

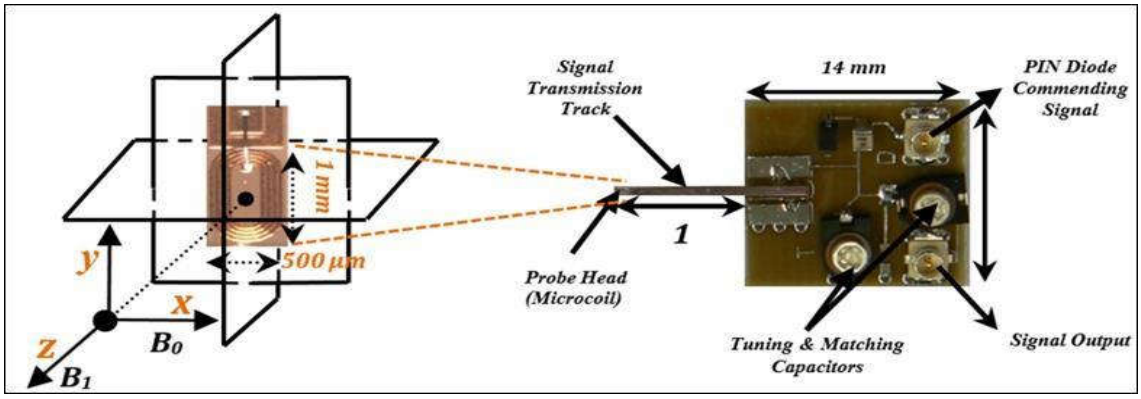

Fig.1. NMR system

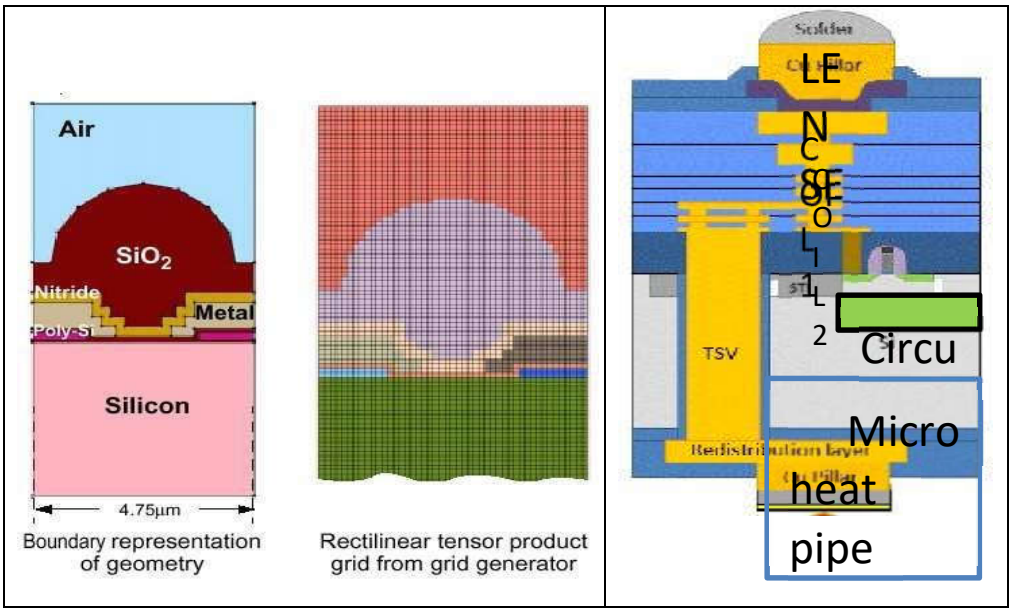

Fig.2. 2D device simulation; from left to right; geometry, meshing, connectics (TSV: Through Silicon Via, RDL… and circuits, embedded into the substrate).

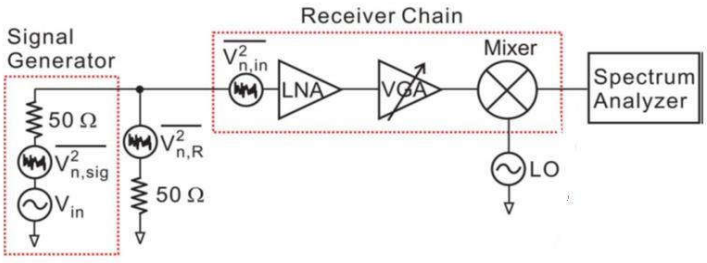

Fig.3. the receiver

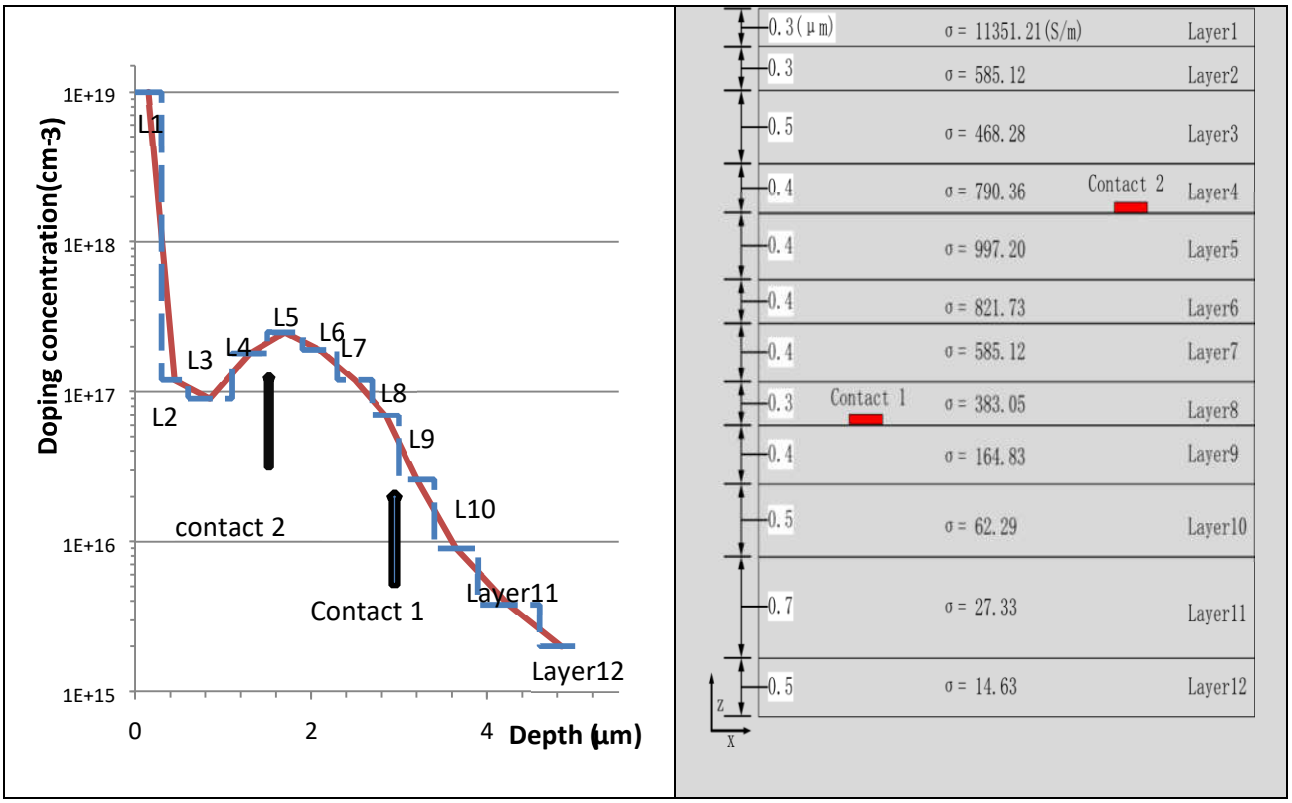

(a) (b)

Fig.4 a. Specific depth profile of a .35m technology (p-region). B; Thicknesses and conductivities

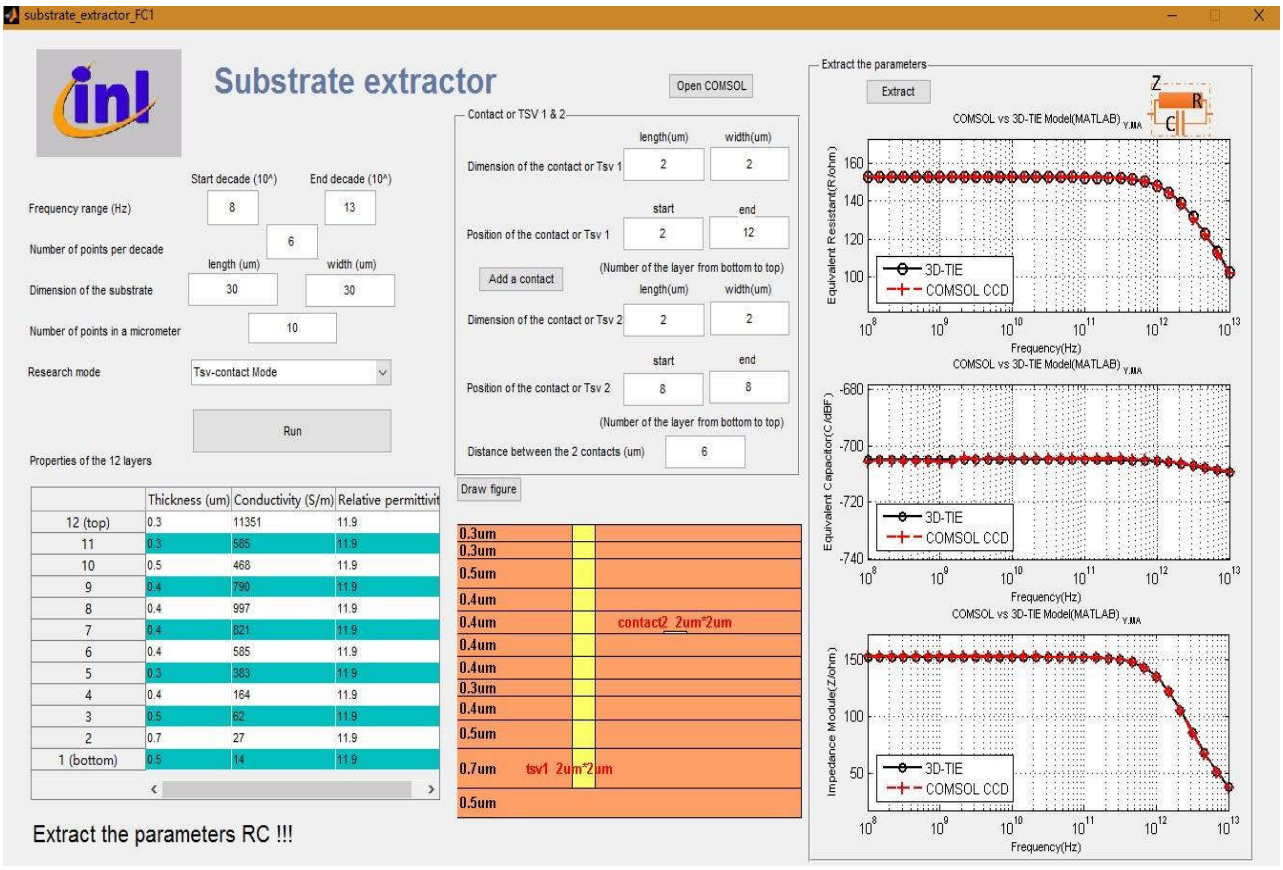

Fig.5. Example: Impedance Z_{17}, capacitance and résistance C_{17} ET R_{17n}.extracted between One contract and one TSV

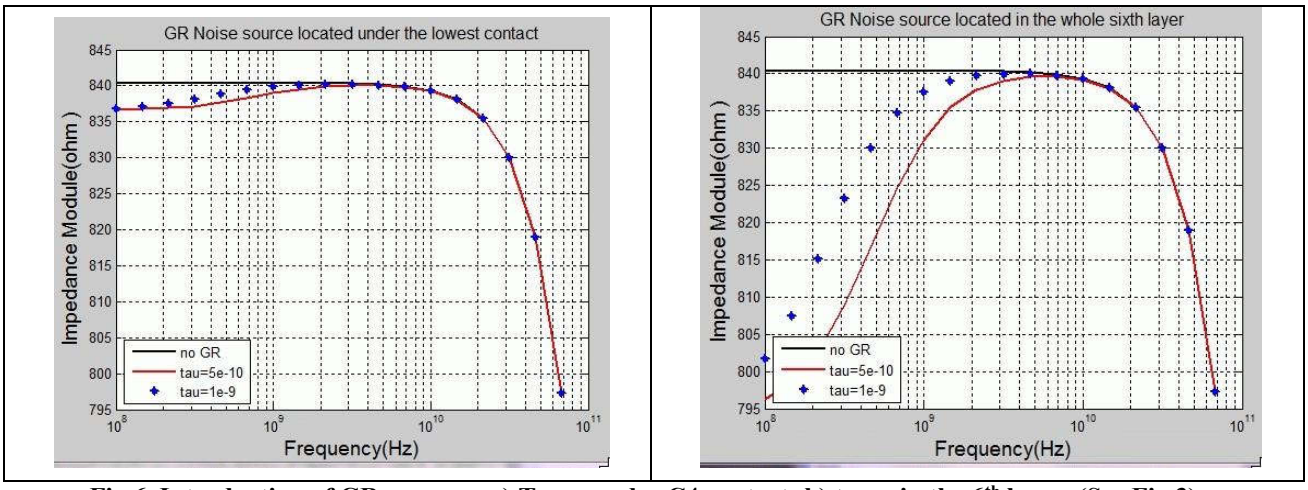

Fig.6. Introduction of GR process. a) Traps under C4 contact; b) traps in the 6th layer. (See Fig.3)

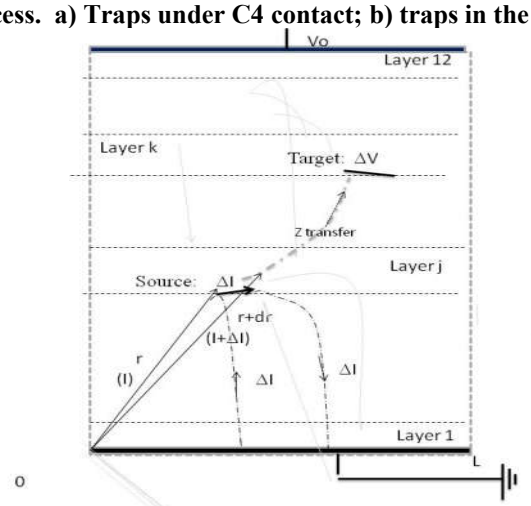

Fig. 7. Schematic of the principle of the impedance field method.

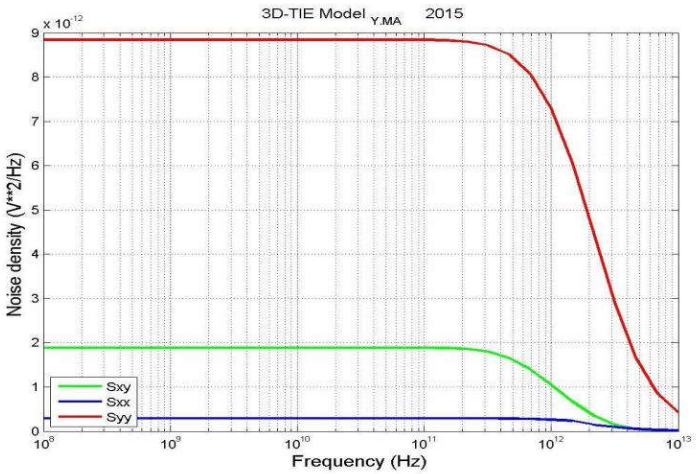

Fig. 8. Spectral Noise density.

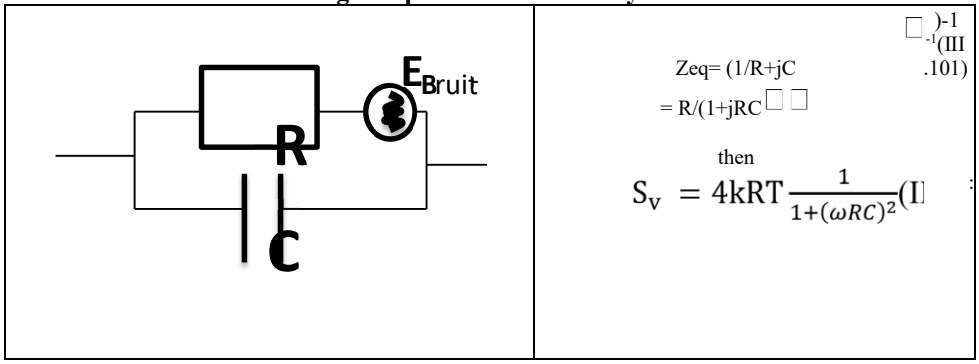

Fig. 9. Equivalent noise model for any substrate layer

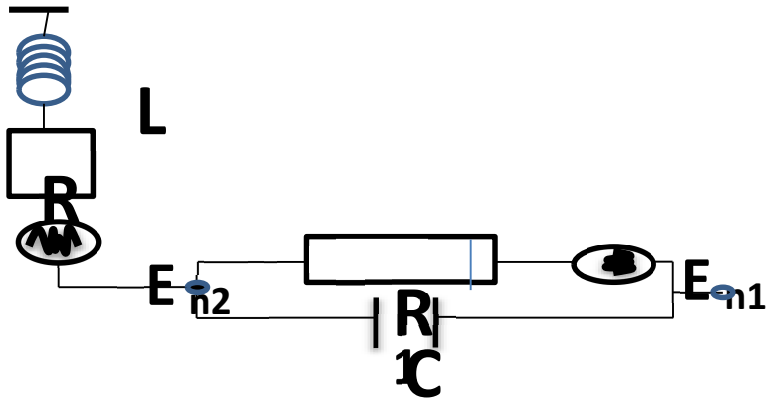

Fig.10 (L, R) and (R, C) noisy dipoles

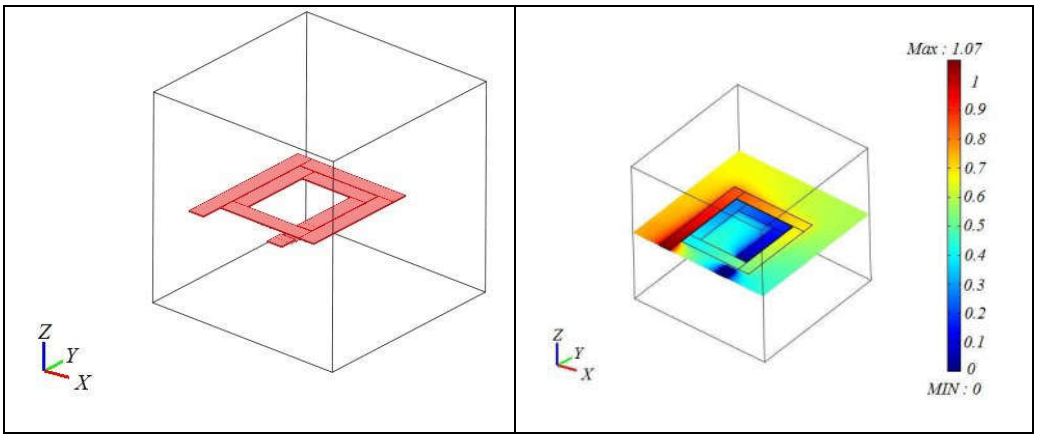

Fig.11. Left; geometric description of the inductance (COMSOL [8])
Right: Electrostatic potential for the polarizedinductance.

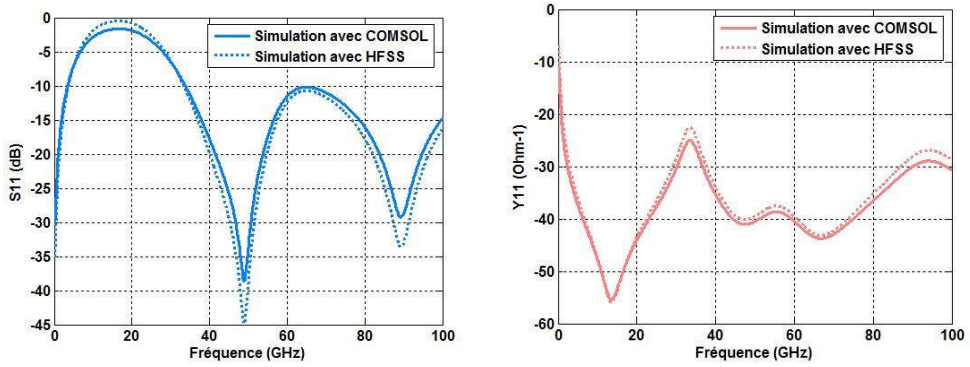

Fig. 12 Left: Reflection parameter, Right: Admittance versus the frequency

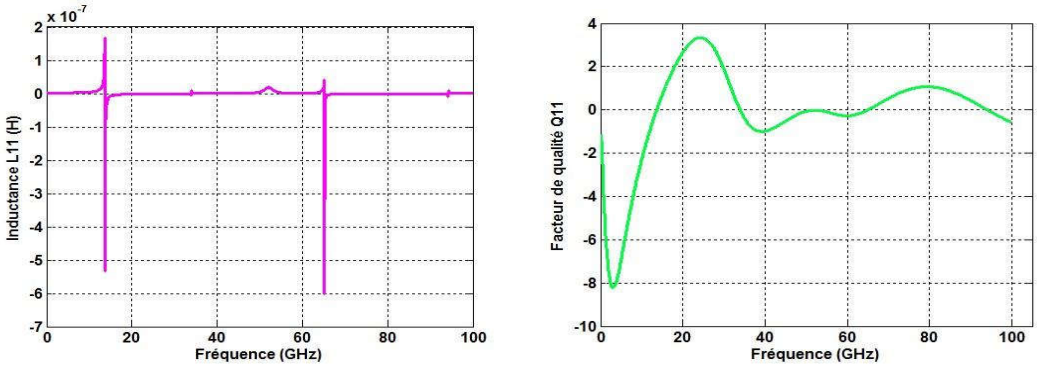

Fig. 13: Left) Inductance and Right) quality factor, versus the frequency